ELSEVIER

Catalysis Today 85 (2003) 13–21

CATALYSIS TODAY

www.elsevier.com/locate/cattod

# The role of Ni on the performance of automotive catalysts: evaluating the ethanol oxidation reaction

Fábio B. Noronha, Marcelo C. Durão, Marcelo S. Batista, Lucia G. Appel*

*Laboratório de Catálise, Instituto Nacional de Tecnologia/MCT, Av. Venezuela 82 sala 518, CEP 20081-310, Centro, Rio de Janeiro, Brazil*

## Abstract

The role of the nickel oxide on the ethanol oxidation reaction over different model catalysts and commercial catalyst was studied. At 473 K, the catalytic activity followed the order: $Pd/Al_2O_3 \approx Pd/CeO_2/Al_2O_3 \approx Pd/Al_2O_3 + NiO/Al_2O_3$ physical mixture $> Pd/NiO/Al_2O_3 \approx Pd/NiO/CeO_2/Al_2O_3 \approx$ commercial catalyst. $NiO/Al_2O_3$ and $CeO_2/Al_2O_3$ catalysts were not active at this temperature. Nickel addition strongly decreased the catalytic activity of $Pd/Al_2O_3$ and $Pd/CeO_2/Al_2O_3$ catalysts. Temperature-programmed reduction (TPR) and oxygen storage capacity (OSC) measurements showed that palladium promoted the nickel oxide reduction. This strong interaction between both metals was destroyed under the reaction conditions leading to a nickel oxide surface segregation. The decrease of ethanol conversion in the presence of nickel was due to the coverage of palladium particles by nickel oxide, as demonstrated by IR analysis. The catalytic behavior of commercial catalyst was well represented by the $Pd/NiO/CeO_2/Al_2O_3$ model catalyst. The main products of ethanol oxidation were acetaldehyde, acetic acid, carbon oxides and ethyl acetate. Ethanol oxidation proceeds through parallel and series reactions. The nickel addition shifted all the reaction system towards high temperature due to the decrease of activity.

*Keywords:* Automotive catalysts; Pd-Ni catalysts; Ethanol oxidation

## 1. Introduction

All commercially produced gasoline blends contain organo-sulfur compounds in concentrations up to 1000 ppm [1]. Combustion of a fuel containing sulfur compounds results in the formation of $SO_2$ and $SO_3$, which can deactivate vehicle exhaust catalysts [1,2]. Several studies were carried out to investigate the effects of sulfur as well as the mechanism of sulfur poisoning of three-way catalysts (TWC) [1,3–5]. Beck and Sommers reported that the activity for hydrocarbon (HC) and $NO_x$ is deteriorated in the presence of sulfur [1]. $SO_2$ formed can also be reduced to $H_2S$ under specific vehicle operating conditions [6,7]. To reduce $H_2S$ emissions, catalysts manufactures have used different additives to catalyst formulation such as NiO, $Fe_2O_3$ [8].

Nickel plays a role of a regenerable $H_2S$-trap, which retains $H_2S$ formed under rich conditions and is re-activated under lean atmosphere [6]. This mechanism involves the formation of $NiSO_4$ under fuel-lean atmosphere. However, these additives can also reduce the activity of TWC [7]. It is suggested that the catalyst deactivation is inhibited by minimizing the interaction between the TWC and nickel compound. Andersen et al. [7] studied the mechanism of Ni deactivation of TWC. According to the authors, the catalyst deactivation under redox (cycled reducing/oxidizing) aging was due to the formation of Pd–Ni alloy.

---

* Corresponding author. Fax: +55-21-2263-6552.
*E-mail address:* appel@uol.com.br (L.G. Appel).

0920-5861/$ – see front matter © 2003 Elsevier B.V. All rights reserved.
doi:10.1016/S0920-5861(03)00189-5

In addition to the high sulfur level, the Brazilian gasoline has also around 20% of ethanol. The use of ethanol as fuel or fuel additives can reduce the emission of conventional pollutants such as carbon monoxide. On the other hand, the use of ethanol increased the direct emissions of unburned ethanol, acetaldehyde and $NO_x$ [9]. Aldehydes in the atmosphere have been associated with a number of health effects such as eye, nose and throat irritation, asthma attacks, and a potential human carcinogen [10]. It is well known that these compounds also participate in atmospheric photochemical reactions that lead to the formation of peroxyacetil nitrate [11].

Therefore, it is necessary that the usual catalytic converter is able to control the emission of these compounds. Pd-Mo/$Al_2O_3$ catalysts were initially used to control the exhaust emissions of ethanol-fueled Brazilian vehicles. It has been reported that the addition of $MoO_3$ to Pd/$Al_2O_3$ catalysts improves the NO activity with high selectivity to $N_2$ [12–14]. Recently, Pd-Mo/$Al_2O_3$ catalysts were studied for the CO + NO [15–17], ethanol + NO [17] and acetaldehyde + NO [18] reactions. A redox mechanism was proposed to explain the molybdenum promoting effect on Pd in the CO + NO reaction. On the other hand, molybdenum oxide does not promote the ethanol + NO reaction and this was attributed to different reaction mechanism. Pd-Mo/$Al_2O_3$ catalyst showed higher activity for the reduction of NO by acetaldehyde than Pd catalyst. However, the selectivity to $N_2$ was nearly the same, indicating that the mechanism was the same on both catalyst.

Nevertheless, there is no information about the effect of oxygenated organic compounds on the catalytic properties of Pd based catalysts containing Ni. The aim of this work is to investigate the role of Ni on the ethanol oxidation over model and commercial automotive catalyst.

## 2. Experimental

### 2.1. Catalyst preparation

$Al_2O_3$ support was prepared by calcination of a γ-alumina (Engelhard, AL-3916P) at 823 K, for 16 h in a muffle. Pd/$Al_2O_3$, NiO/$Al_2O_3$ and $CeO_2$/$Al_2O_3$ samples were prepared by dry impregnation of alumina with an aqueous solution of $PdCl_2$, $Ni(NO_3)_2$, $Ce(NO_3)_3$, respectively. The solids were dried at 343 K, for 16 h and calcined at 773 K, for 2 h (2 K/min) under air flow. Pd/NiO/$Al_2O_3$, Pd/$CeO_2$/$Al_2O_3$ and NiO/$CeO_2$/$Al_2O_3$ samples were prepared by impregnation of NiO/$Al_2O_3$ and $CeO_2$/$Al_2O_3$ samples using the same procedure and precursors salts describe above. Pd/NiO/$CeO_2$/$Al_2O_3$ was also obtained by dry impregnation of NiO/$CeO_2$/$Al_2O_3$ by using $PdCl_2$ as precursor and the same thermal treatment described above. A physical mixture of Pd/$Al_2O_3$ and NiO/$Al_2O_3$ (1:1 (w/w)) was prepared in an agate mortar. The commercial catalyst was made by hand-grinding in an agate mortar. The Ce, Ni and Pd concentration of the model catalyst and of the commercial catalyst are displayed on Table 1.

Table 1
Ce, Ni and Pd content on the prepared and commercial catalysts (without cordierita)

| Catalysts | Concentration (wt.%) | | |
|---|---|---|---|
| | Pd | NiO | $CeO_2$ |
| Pd/$Al_2O_3$ | 0.92 | – | – |
| NiO/$Al_2O_3$ | – | 12.36 | – |
| Pd/NiO/$Al_2O_3$ | 0.94 | – | – |
| Pd/$CeO_2$/$Al_2O_3$ | 0.85 | – | 33.25 |
| Pd/NiO/$CeO_2$/$Al_2O_3$ | 0.88 | 12.89 | 28.47 |
| Commercial | 0.93 | 13.07 | 32.39 |

### 2.2. Catalyst characterization

#### 2.2.1. Temperature-programmed reduction (TPR)

Temperature-programmed reduction (TPR) experiments were performed in a conventional apparatus, as described previously [19]. Before reduction, the catalysts were heated at 423 K in flowing nitrogen for 0.5 h. Then, a mixture of 4.7% hydrogen in nitrogen was passed through the sample and the temperature was raised from 298 up to 773 K at a heating rate of 10 K/min.

#### 2.2.2. Oxygen storage capacity measurements (OSC)

A pulse technique was used to determine the oxygen storage capacity (OSC) of the samples [20]. The catalyst (300 mg) was oxidized at 873 K, for 1 h, under air flow and cooled to 703 K under nitrogen for

30 min. Then, the sample was reduced at 703 K under a 5% $H_2$ in $N_2$ (AGA) mixture (30 ml/min). Oxygen pulses (0.20 ml) were then performed at the same temperature.

#### 2.2.3. Infrared spectroscopy analysis

Infrared spectroscopy analyses were performed in a Magna 750-Nicolet apparatus. Each wafer contained approximately 5 mg of catalyst diluted in 40 mg of α-alumina. The samples were dried under $N_2$ at 423 K, during 1 h, reduced with $H_2$ at 773 K, for 1 h, and exposed to high vacuum during 1 h. After exposition to the reaction mixture at 393 K, during 5 h, a primary vacuum was carried out during 15 min. The sample was then cooled to room temperature and spectra were recorded. Afterwards, the sample was heated to another temperature under the reaction mixture and the procedure previously described was repeated.

### 2.3. Catalytic tests

The catalytic tests were performed in a quartz reactor at atmospheric pressure and the products were monitored by on-line gas chromatography, with flame ionization and conductivity detectors. Prior to reaction, the sample (28 mg of catalyst diluted in 120 mg of SiC) were reduced under $H_2$ at 773 K, for 1 h. Then, a 2% ethanol in air mixture ($O_2/C_2H_5OH$ ratio of 6) obtained by passing air through a saturator containing ethanol at 283 K was fed to the catalyst at the space velocity of 11,520 $h^{-1}$. No deactivation of the catalysts was observed during the study. In order to have the same amount of Pd in all catalytic test, 57 and 86 mg of physical mixture and commercial catalyst was used, respectively.

## 3. Results and discussion

### 3.1. Temperature-programmed reduction (TPR)

TPR profiles of $Pd/Al_2O_3$, $NiO/Al_2O_3$ and $CeO_2/Al_2O_3$ catalysts are presented in Fig. 1. $Pd/Al_2O_3$ exhibited one peak at 406 K. The reduction profile of $NiO/Al_2O_3$ showed one peak at 583 K and a $H_2$ uptake at high temperature, presenting maxima around 994 and 1106 K. The $CeO_2/Al_2O_3$ catalyst displayed a small hydrogen consumption around 789 K and a peak at 1194 K.

According to the literature, the hydrogen consumption at 406 K has been attributed to the reduction of $PdO_xCl_y$ species [21]. In the case of $NiO/Al_2O_3$ catalyst, three reduction regions were identified: region I (570 K), region II (700–900 K) and region III (1020–1150 K) [22]. The first one was assigned to the nitrate decomposition. The second region corresponded to the reduction of $Ni^{2+}$ species highly dispersed. This region was typical of catalysts containing high Ni content calcined at low temperature. The last one was due to the reduction of a $NiAl_2O_4$ phase formed by the diffusion of Ni ions into the support and was mainly observed on catalysts calcined at high temperature. Therefore, in our work, the TPR profile of $NiO/Al_2O_3$ catalyst revealed the presence of nickel nitrate, $Ni^{2+}$ species highly dispersed and nickel aluminate. Monteiro et al. [23] also performed TPR analysis on $CeO_2/Al_2O_3$ samples with different ceria loading. TPR profiles of 3 and 20% $CeO_2/Al_2O_3$ showed several reduction peaks at around 720, 870, 1135 and above 1150 K. The relative intensity of these peaks were related to ceria loading. In the literature, these peaks have been ascribed to different ceria species. According to Shyu et al. [24], the peak at around 720 K corresponds to reduction of ceria capping oxygen. The peaks at 870, 1000 and above 1200 K were assigned to the formation of non-stoichiometric cerium oxides ($CeO_x$), $CeAlO_3$ and $Ce_2O_3$, respectively. Appel et al. [25] studied the influence of the precursor, calcination temperature and cerium content on distribution of cerium species over alumina. TPR results also revealed the presence of several reduction peaks, which were attributed to the surface reduction of $CeO_2$ and to the formation of $CeAlO_3$ and $Ce_2O_3$. According to the literature, in this work the $H_2$ uptake corresponded to the reduction of ceria capping oxygen (867 K) and the formation of $Ce_2O_3$ (1160 K).

Fig. 2 exhibited the TPR profiles of the $Pd/NiO/Al_2O_3$, $Pd/CeO_2/Al_2O_3$, $NiO/CeO_2/Al_2O_3$ and $Pd/NiO/CeO_2/Al_2O_3$ catalysts.

The TPR profile of $Pd/NiO/Al_2O_3$ showed three peaks at 431, 729 and 979 K. It is important to stress that the TPR profile of $Pd/NiO/Al_2O_3$ did not correspond to the addition of the reduction of monometallic catalysts. These results suggested the

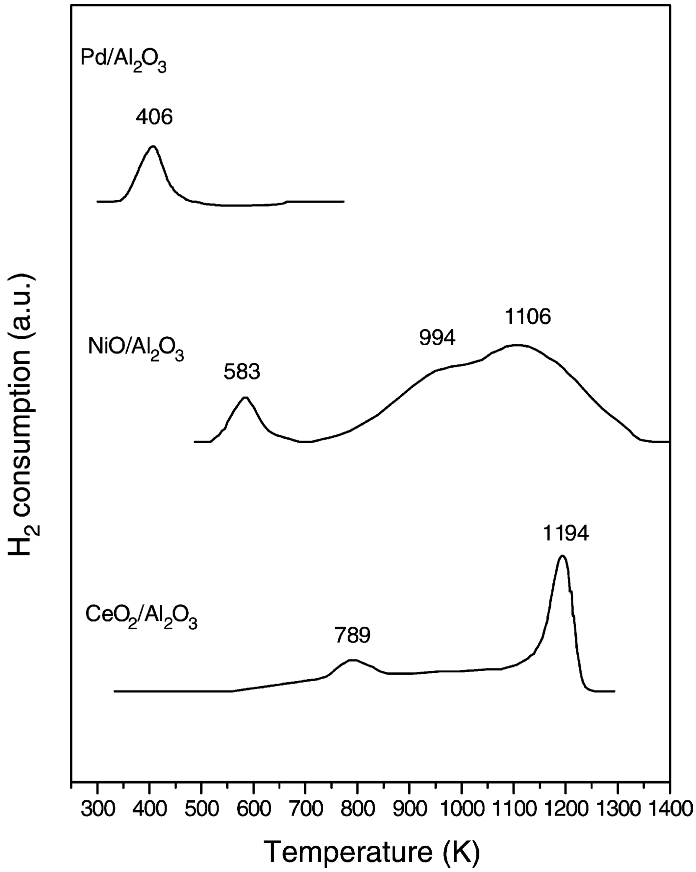

Fig. 1. TPR profile of $Pd/Al_2O_3$, $NiO/Al_2O_3$, $CeO_2/Al_2O_3$.

existence of an interaction between both metals. The peak at 431 K corresponded not only to palladium oxide reduction but also to nickel nitrate since the hydrogen consumption was higher than the one on the $Pd/Al_2O_3$ (Table 2). Furthermore, the presence of palladium shifted the peaks associated to the reduction of superficial $Ni^{2+}$ and nickel aluminate to lower temperatures. Therefore, the palladium addition to $NiO/Al_2O_3$ catalyst promoted the reduction of nickel oxides. These results suggested the presence of a strong interaction between palladium and nickel oxide.

Two peaks at 381 and 1148 K and a hydrogen uptake between 700 and 1200 K were observed on the TPR profile of $Pd/CeO_2/Al_2O_3$ catalyst. The peak at 381 K was ascribed to palladium oxide reduction whereas the hydrogen uptake at high temperatures was due to the formation of $Ce_2O_3$. However, the hydrogen consumption at 381 K was higher than that necessary to reduce the palladium oxide (Table 2) suggesting that reduction of ceria capping oxygen occurred at this region. Therefore, the palladium addition promoted the

Table 2
$H_2$ consumption during TPR

| Catalysts | $H_2$ consumption ($\mu$mol/$g_{cat}$) | | |
|---|---|---|---|
| | Total | First peak | First peak-Pd[a] |
| $Pd/Al_2O_3$ | 45 | 45 | – |
| $CeO_2/Al_2O_3$ | 737 | 182 | – |
| $Pd/CeO_2/Al_2O_3$ | 798 | 273 | 228 |
| $NiO/Al_2O_3$ | 1483 | 122 | – |
| $Pd/NiO/Al_2O_3$ | 1450 | 155 | 110 |
| $NiO/CeO_2/Al_2O_3$ | 2189 | | – |
| $Pd/NiO/CeO_2/Al_2O_3$ | 2275 | | |

[a] $H_2$ consumption of the first peak removing the palladium oxide reduction.

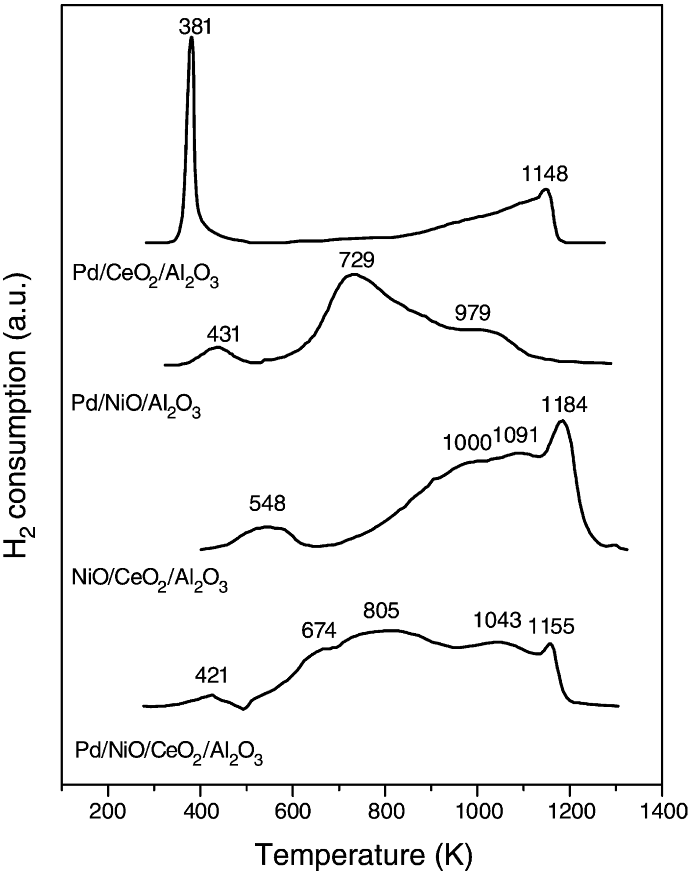

Fig. 2. TPR profile of $Pd/NiO/Al_2O_3$, $Pd/CeO_2/Al_2O_3$, $NiO/CeO_2/Al_2O_3$ and $Pd/NiO/CeO_2/Al_2O_3$ samples.

reduction of cerium oxide species, in agreement with Monteiro et al. [23].

The TPR profile of $NiO/CeO_2/Al_2O_3$ catalyst displayed three peaks at 548, 1091 and 1184 K and a shoulder around 1000 K. This profile was very similar to the ones of the monometallic catalysts, indicating that the presence of nickel oxide did not promote the cerium oxide reduction.

The $Pd/NiO/CeO_2/Al_2O_3$ catalyst exhibited a very complex TPR profile, with peaks at 421, 674, 805, 1043 and 1155 K. A comparison to the TPR of $NiO/CeO_2/Al_2O_3$ catalyst suggested that the palladium addition also promoted the reduction of the species presented on the $NiO/CeO_2/Al_2O_3$ catalyst due to the shift of the reduction regions to lower temperatures.

Therefore, these TPR results revealed that palladium addition had an important promoting effect on the reduction of both NiO and $CeO_2$. According to [23], hydrogen is activated on metallic palladium through dissociative adsorption to atomic hydrogen, which promotes the reduction of metal oxide.

### 3.2. Oxygen storage capacity measurements (OSC)

The OSC values of the samples are displayed in Fig. 3. The oxygen storage capacity of $Pd/Al_2O_3$ sample was slightly higher than the one of $CeO_2/Al_2O_3$. TPR results indicated that oxygen consumption of OSC measurements was associated to the oxidation of completely reduced Pd whereas the OSC value of $CeO_2/Al_2O_3$ sample corresponded to the re-oxidation

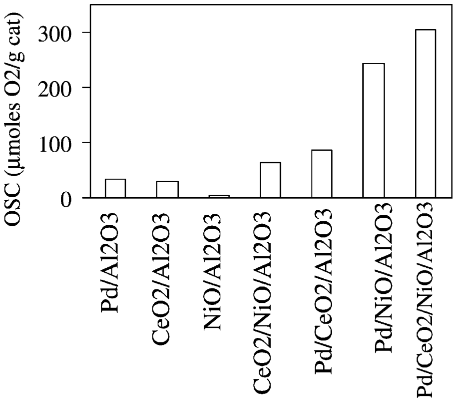

Fig. 3. Oxygen storage capacity (OSC) values of the samples.

of superficial cerium oxide species. The oxygen storage capacity of $NiO/Al_2O_3$ was indeed very low. In this case, the pretreatment before the OSC analysis decomposed the nickel nitrate residues but it was not able to reduce the nickel oxide species. According to TPR analysis, their reduction took place at higher temperatures.

For the $CeO_2/NiO/Al_2O_3$ sample, the OSC value corresponded practically to the sum of the oxygen uptake on $NiO/Al_2O_3$ and $CeO_2/Al_2O_3$ samples. This result agreed very well to the TPR profiles which did not detect the presence of an interaction between Ni and Ce on this catalyst.

The OSC value of $Pd/CeO_2/Al_2O_3$ sample was higher than that obtained by the addition of $Pd/Al_2O_3$ and $CeO_2/Al_2O_3$ OSC values. Taking into account the TPR results, it can be suggested that the $CeO_2$ reduction is related not only to the superficial oxygen but also to the oxygen from sublayers of the $CeO_2$ structure. Indeed, it is well known that $CeO_2$ is able to release and get oxygen atoms without significant changes in its crystalline structure [26]. This behavior is promoted by Pd at low temperatures.

As for $Pd/NiO/Al_2O_3$, the palladium addition to $Ni/Al_2O_3$ sample strongly increased the OSC value. In accordance to TPR analysis, this result can be assigned to the promoted reduction of $Ni^{2+}$ dispersed species. Furthermore, the $Pd/NiO/Al_2O_3$ sample had an OSC value higher than $Pd/CeO_2/Al_2O_3$ sample. This result is connected to the intrinsic redox properties of each metal oxide, which produced different oxygen consumption. During OSC measurements, $Ni^0$ and $Ce^{3+}$ formed during pretreatment were oxidized to $Ni^{2+}$ and $Ce^{4+}$, respectively. This change in oxidation state corresponds to a more important oxygen uptake on the nickel based catalyst. Lööf et al. [27] reported the same behavior on a commercial catalyst.

It is worth noting that the OSC value of $Pd/NiO/CeO_2/Al_2O_3$ is smaller than the addition of $Pd/NiO/Al_2O_3$ and $Pd/CeO/Al_2O_3$ ones. This result is related to the fact that the three samples have the same Pd concentration, i.e. 1 wt.%. Thus the contact between palladium and metal oxides is smaller on the catalyst containing both additives.

### 3.3. Infrared spectroscopy analysis

Fig. 4 exhibited the infrared spectra after ethanol oxidation at different temperatures on $Pd/Al_2O_3$,

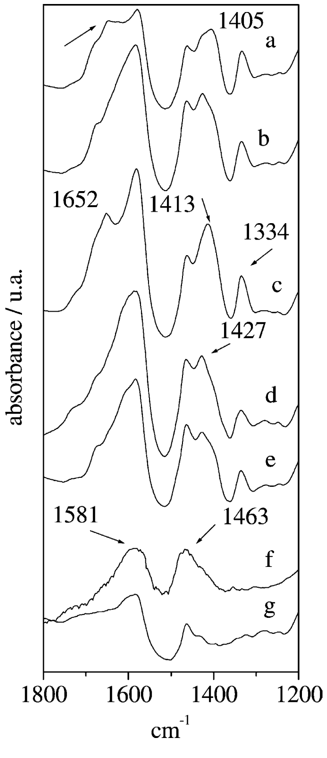

Fig. 4. Infrared spectra after ethanol oxidation at different temperatures on the catalysts—$Pd/Al_2O_3$: (a) 393 K, (c) 513 K, (f) 603 K; $Pd/NiO/Al_2O_3$: (b) 393 K, (d) 513 K, (g) 603 K; $NiO/Al_2O_3$: (e) 513 K.

$NiO/Al_2O_3$ and $Pd/NiO/Al_2O_3$ catalysts. It is important to stress that no signal related to the adsorption of ethanol on alumina support was observed.

After reaction at 393 K (Fig. 4a), the IR spectrum on $Pd/Al_2O_3$ presented the following bands: 1581, 1463, 1405 and 1334 $cm^{-1}$ and also shoulders at 1427 and 1652 $cm^{-1}$. The same bands can be observed after the reaction at 513 K (Fig. 4c). However, the intensity of bands at 1652 and 1405 $cm^{-1}$ decreased whereas the intensity of the bands at 1413 $cm^{-1}$ increased. After reaction at 603 K, only two bands at 1581 and 1463 $cm^{-1}$ were noted (Fig. 4f).

Medeiros et al. [28] studied the ethanol oxidation on Mo-Sn catalysts using the same procedure of this work. At room temperature, they observed the presence of bands around 1450, 1390, 1266, 1089, 1042 $cm^{-1}$, which were assigned to ethoxy species. After reaction at 473 K, the appearance of bands at 1527, 1435, 1387 and 1320 $cm^{-1}$ was associated to bridged and monodented carboxylate. However, only the bands characteristic of bridged carboxylate (1527 and 1435 $cm^{-1}$) were observed after reaction at high temperature (543 K).

Baldanza et al. [17] performed FTIR analyses of adsorbed ethanol on $Al_2O_3$ and $Pd/Al_2O_3$. The results revealed the presence of bands characteristics of ethoxy species at 1447, 1389, 1168, 1120, 1075 $cm^{-1}$. Bands at 1585 and 1463 $cm^{-1}$ were attributed to the asymmetric and symmetric stretching acetate species, respectively, in agreement with [29]. As the temperature was raised, the band intensity of the ethoxy species decreased while the band intensity related to acetate species increased.

A comparison with literature data indicates that the band at 1405 $cm^{-1}$ is associated to ethoxy species. The other bands can be attributed to carboxylate species.

In the case of $Pd/NiO/Al_2O_3$ and $NiO/Al_2O_3$ catalysts (Fig. 4b, d and e), the IR spectra were very similar to the one of $Pd/Al_2O_3$ catalyst. However, there are some differences that are worth to point out. On $Pd/Al_2O_3$ catalyst, the intensities of the bands around 1652 and 1413 $cm^{-1}$ were higher than on the catalysts containing Ni. These vibrations corresponded to bridged carboxylates due to their position and $\Delta\nu$. The bands at 1334 and 1427 $cm^{-1}$ were associated to monodented carboxylates [28–30].

After reaction at high temperature (603 K), the IR spectra of $Pd/Al_2O_3$ and $Pd/NiO/Al_2O_3$ were even more similar (Fig. 4f and g). Taking into account the high stability of these species (1581 and 1463 $cm^{-1}$), they could be assigned to asymmetric and symmetric—$CO_2$ stretching modes of bridged carboxylates.

Therefore, during ethanol oxidation on $Pd/Al_2O_3$, $NiO/Al_2O_3$ and $Pd/NiO/Al_2O_3$ catalysts, it was observed the formation of ethoxy species and bridged carboxylates, which are $CO_2$ precursors and monodented carboxylate, which are related to acetic acid and ethyl acetate production.

Furthermore, the bands at 1652 and 1413 $cm^{-1}$ were characteristic of palladium since their intensity was very low on the nickel based catalyst. It means that the decrease of the intensity of the bands at 1652 and 1413 $cm^{-1}$ on $Pd/NiO/Al_2O_3$ catalyst is probably due to the coverage of palladium particles by nickel atoms.

### 3.4. Catalytic activity

Fig. 5 displays the curves related to the conversion of ethanol at different reaction temperatures. $NiO/Al_2O_3$ and $NiO/CeO_2/Al_2O_3$ catalysts showed very low activity. These systems were not active at 473 K whereas the ethanol conversion was almost complete on the Pd based catalysts at the same temperature.

Ni addition to $Pd/Al_2O_3$ and $Pd/CeO_2/Al_2O_3$ catalysts strongly decreased their activity. Andersen et al. [7] reported the same behavior on three-way catalysts in the presence of nickel. According to the authors, the catalyst deactivation under redox (cycled reducing/oxidizing) aging was due to the formation of Pd–Ni alloy. They suggested that the catalyst deactivation is inhibited by minimizing the interaction between the TWC and nickel compound. In our work, TPR analysis showed that palladium addition promoted the nickel oxide reduction, which indicated the presence of a strong interaction between both metals. Under the slightly oxidizing conditions of the catalytic test, this interaction could be destroyed and a strong segregation of one of the components at the surface could take place. In fact, the IR analysis revealed the coverage of metallic palladium particles by nickel oxide, which were not active. This could be responsible for the decrease of the ethanol conversion observed on the bimetallic catalyst. This is also confirmed by the catalytic behavior of the $Pd/Al_2O_3 + NiO/Al_2O_3$

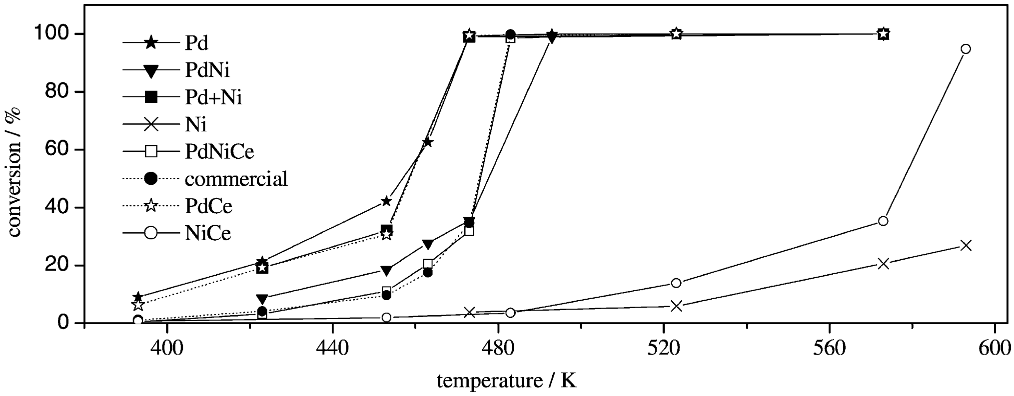

Fig. 5. Conversion of ethanol as a function of reaction temperature on model and commercial catalysts.

physical mixture. In this case, the physical mixture exhibited the same activity than the Pd/$Al_2O_3$ catalyst, since there was no interaction between both metals. Therefore, in order to minimize the negative effect of nickel addition to palladium based catalysts on ethanol oxidation reaction, it is important to inhibit the interaction between palladium and nickel.

Finally, the commercial catalyst showed the same results as Pd/NiO/$CeO_2$/$Al_2O_3$ catalysts. This result suggested that the commercial catalyst could be well represented by the Pd/NiO/$CeO_2$/$Al_2O_3$ model catalysts.

The main products of ethanol oxidation were acetaldehyde, acetic acid, carbon oxides and ethyl acetate, as it is shown in Figs. 6 and 7. It is worth to stress that the products of partial oxidation are only observed at conversion levels of ethanol below 100%. The curves clearly indicated that acetaldehyde was the primary product; which was subsequently oxidized to acetic acid and carbon oxides. The reaction between acetaldehyde and ethoxy species might produce ethyl acetate. In accordance with [31], ethanol oxidation is represented by a system of parallel and series reactions. The presence of Ni shifted all the reaction system towards high temperature (Fig. 7). This result agrees with the decrease of activity shown in Fig. 6. Moreover, the presence of Ni decreased the selectivity towards ethyl acetate, which is probably due to the modification of the acid and basic properties of the support.

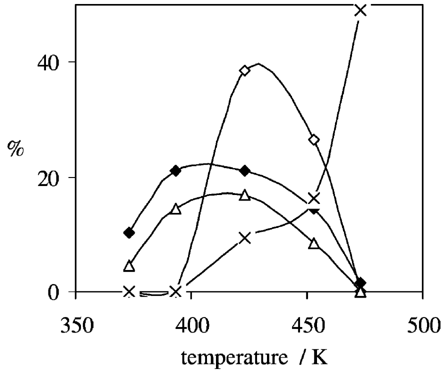

Fig. 6. Selectivities on the ethanol oxidation as a function of temperature on Pd/$Al_2O_3$ catalyst. (◆) Acetaldehyde; (◇) acetic acid; (×) $CO_2$; (△) ethyl acetate. Selectivity is defined as the ratio between the amount of ethanol converted to a product and the reacted amount of ethanol.

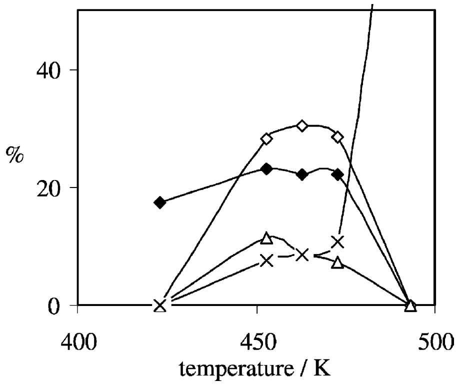

Fig. 7. Selectivities on the ethanol oxidation as a function of temperature on Pd/NiO/$Al_2O_3$ catalyst. (◆) Acetaldehyde; (◇) acetic acid; (×) $CO_2$; (△) ethyl acetate.

## 4. Conclusion

In order to study the role of nickel oxide on ethanol oxidation, several model catalysts were prepared: $Pd/Al_2O_3$, $NiO/Al_2O_3$, $CeO_2/Al_2O_3$, $Pd/CeO_2/Al_2O_3$, $Pd/NiO/Al_2O_3$, $Pd/NiO/CeO_2/Al_2O_3$, $Pd/Al_2O_3 + NiO/Al_2O_3$ physical mixture. A commercial catalyst was also studied.

TPR and OSC measurements revealed that palladium addition strongly promoted the reduction of cerium oxide and nickel oxide. This effect was more important on $Pd/NiO/Al_2O_3$ catalyst, suggesting the presence of a strong interaction between palladium and nickel.

$Pd/Al_2O_3$ and $Pd/CeO_2/Al_2O_3$ catalysts exhibited practically the same catalytic activity. On the other hand, the presence of nickel decreased the ethanol conversion. Under the slightly oxidizing reaction conditions, the interaction between both metals was destroyed. The IR analyses showed evidences of a surface segregation of nickel oxide, which were not active. This could explain the low activity of the nickel based bimetallic catalysts. In order to minimize the negative effect of nickel addition to palladium based catalysts on ethanol oxidation reaction, it is important to inhibit the interaction between palladium and nickel.

The ethanol oxidation produced mainly acetaldehyde, acetic acid, carbon oxides and ethyl acetate. The addition of nickel shifted the formation of these products towards higher temperature due to the decrease of activity.

A commercial catalyst was also tested and compared to the model catalysts. The commercial catalyst presented catalytic activity similar to the $Pd/NiO/CeO_2/Al_2O_3$ catalyst. This result suggested that the commercial catalyst could be well represented by this model catalyst.

## Acknowledgements

Marcelo C. Durão and Marcelo S. Batista would like to thank CNPq for financial support.

## References

[1] D.D. Beck, J.W. Sommers, Appl. Catal. B: Environ. 6 (1995) 185.
[2] H.S. Gandhi, M. Shelef, Appl. Catal. 77 (1991) 175.
[3] C.E. Lindhjem, SAE Paper 950778, 1995.
[4] A. Datta, R.G. Cavell, R.M. Tower, Z.M. George, J. Phys. Chem. 89 (1985) 443.
[5] D.D. Beck, M.H. Krueger, D.R. Monroe, SAE Paper 910844, 1991.
[6] S.E. Golunski, S. Roth, Catal. Today 9 (1991) 105.
[7] P.J. Andersen, T.H. Ballinger, C.J. Bennett, in: Proceedings of the 17th North American Catalysis Society Meeting, Toronto, Canada, p. 141, 2001.
[8] P. Degobert, Automobiles and Pollution, SAE Inc., Éditions Technip, Paris, 1995.
[9] D.A. Guerrieri, P.J. Caffrey, V. Rao, SAE Paper 950777, 1995.
[10] A.P. Altshuller, Atmos. Environ. A 27 (1993) 21.
[11] A.H. Miguel, J.B. Andrade, J. Bras. Chem. Soc. 1 (1990) 124.
[12] H.S. Ghandi, H.C. Yao, H.K. Stepien, in: A.T. Bell, L.L. Hegedus (Eds.), Catalysis Under Transient Conditions, ACS Symposium Series no. 178, 1982, p. 143.
[13] I. Halasz, A. Brenner, M. Shelef, N. Simon, Appl. Catal. A: Gen. 82 (1992) 51.
[14] I. Halasz, A. Brenner, M. Shelef, Appl. Catal. B: Environ. 2 (1993) 131.
[15] M. Schmal, M.A.S. Baldanza, M.A. Vannice, J. Catal. 185 (1999) 138.
[16] F.B. Noronha, M.A.S. Baldanza, M. Schmal, J. Catal. 188 (1999) 270.
[17] M.A.S. Baldanza, L.F. de Mello, F.B. Noronha, M. Schmal, J. Catal. 192 (2000) 64.
[18] L.F. de Mello, F.B. Noronha, M. Schmal, in: Proceedings of the 17th North American Catalysis Society Meeting, Toronto, Canada, 2001, p. 11.
[19] F.B. Noronha, M. Primet, R. Frety, M. Schmal, Appl. Catal. 78 (1991) 125.
[20] C. Leitenburg, A. Trovarelli, J. Llorca, F. Cavani, G. Bini, Appl. Catal. A: Gen. 139 (1996) 161.
[21] F.B. Noronha, D.A.G. Aranda, A.P. Ordine, M. Schmal, Catal. Today 57 (2000) 169.
[22] B. Scheffer, P. Molhoek, J.A. Moulijn, Appl. Catal. 46 (1989) 11.
[23] R.S. Monteiro, F.B. Noronha, L.C. Dieguez, M. Schmal, Appl. Catal. A: Gen. 131 (1995) 89.
[24] J.Z. Shyu, W.H. Weber, H.S. Gandhi, J. Phys. Chem. 92 (1988) 4964.
[25] L.G. Appel, J.G. Eon, M. Schmal, Phys. Stat. Sol. (a) 163 (1997) 107.
[26] A. Laachir, V. Perrichon, A. Badri, J. Lamotte, E. Catherine, J.C. Lavalley, J. El Fallah, L. Hilaire, F. le Normand, E. Quémeré, G.N. Sauvion, O. Touret, J. Chem. Soc., Faraday Trans. 87 (1991) 1601.
[27] P. Lööf, B. Kasemo, K.E. Keck, J. Catal. 118 (1989) 339.
[28] P.R.S. Medeiros, J.G. Eon, L.G. Appel, Appl. Catal. A: Gen. 1–2 (2000) 69.
[29] M. Nagal, R.D. Gonzalez, Ind. Eng. Chem. Prod. Res. Dev. 24 (1985) 5251.
[30] M.I. Zaki, N. Sheppard, J. Catal. 80 (1983) 114.
[31] P.R.S. Medeiros, F. Gonçalves, J.G. Eon, L.G. Appel, Appl. Catal. A 193 (2000) 195.